JOINT EUROPEAN TORUS

JET–P(92)68

E. Thompson, D. Stork, H.P.L. de Esch
and JET Team

The Use of Neutral Beam Heating to Produce High Performance Fusion Plasmas, Including the Injection of Tritium Beams into JET

The Use of Neutral Beam Heating to Produce High Performance Fusion Plasmas, Including the Injection of Tritium Beams into JET

E. Thompson, D. Stork, H.P.L. de Esch and JET Team*

JET-Joint Undertaking, Culham Science Centre, OX14 3DB, Abingdon, UK

** See Annex*

Preprint of Paper to be submitted for publication in
Physics of Fluids B: Plasma Physics

ABSTRACT.

The JET Neutral Beam Injection (NBI) system has proved to be an extremely effective and flexible heating method capable of producing high performance plasmas and performing a wide range of related physics experiments. High fusion performance deuterium plasmas have been obtained in the Hot lon (HI) H-mode regime, using the central particle fuelling and ion heating capabilities of the NBI system in low target density plasmas, and in the Pellet Enhanced Plasma (PEP) H-mode regime, where the good central confinement properties of pellet fuelled plasmas are exploited by additional heating and fuelling as well as the transition to H-mode. The HI H-mode configuration was used for the First Tritium Experiment (FTE) in JET in which NBI was used to heat the plasma using 14 D^0 beams and, for the first time, to inject T^0 using the two remaining beams. These plasmas had a peak fusion power of 1.7MW from D-T fusion reactions. The capability for injection of a variety of beam species (H^0, D^0, $^3He^0$ and $^4He^0$) has allowed the study of confinement variation with atomic mass and the simulation of a-particle transport. Additionally, the use of the NBI system has permitted an investigation of the plasma behaviour near the toroidal limit over a wide range of toroidal field strengths.

1. THE JET NEUTRAL BEAM INJECTION SYSTEM

The NBI system installed on the JET tokamak consists of two injectors, each of which contains 8 beamlines integrated into a single vacuum enclosure[1]. The injection geometry is such that beams from half of the sources can make a double pass through the plasma (the 'tangential' beams) whilst the remaining sources (the 'normal' beams) make a single pass through the plasma. The beams have a radius of tangency of 1.85m (tangential beams) and 1.18m (normal beams) compared to the JET plasma major radius of 2.96m. The original design of the system included the provision to supply beams at voltages of ≤ 80kV or ≤160kV by modifying the configuration of the accelerator structure and associated power supplies of the Positive Ion Neutral Injectors (PINIs) which supply the primary ion beams. The high voltage configuration is chosen to optimise the injected power during the final D-T phase of JET in both deuterium (D^0) and tritium (T^0) by operating at 140kV or 160kV respectively. The various injector configurations used at JET and their performance in terms of beam species, voltage and injected power are given in Table 1. Both injectors have been used to produce powerful long-pulse beams[2] of helium (^3He and ^4He). These have been used not only to produce high performance fusion plasmas with much reduced neutron yields and consequent induced activation of the JET apparatus, but also to make specific contributions to the overall physics programme of JET as described below. Finally, two PINIs have been used to inject energetic T^0 beams for the first time into a tokamak plasma heated by D^0 beams[3].

As a result of a continuous programme of improvements, the ***availability*** defined as the integrated fraction of the total system available for use is presently > 90%. In addition, the ***reliability*** defined as the ratio of total beam energy (MJ) injected into the plasma to the requested value, is also ≥ 90%. A discussion of the technical aspects of this improved reliability is found in reference 4.

2. CONTRIBUTIONS TO THE JET PHYSICS PROGRAMME

The NBI system has the ability to provide high power heating of differing ion species simply and reliably to essentially all magnetic configurations of JET. These include limiter discharges up to 7MA and single and double null X-point configurations (SNX and DNX) up to 5MA[5,6].

Injection into plasmas generated at low values of toroidal magnetic field, has been exploited to produce the highest values of β_T (plasma pressure relative to the toroidal magnetic field pressure).

The application of NBI as a fuelling mechanism has been used to measure, in separate experiments, the particle confinement of helium and tritium ions.

2.1 Variation of energy and particle confinement with atomic mass

By injecting the same species as that of the target plasma ($H^0 \rightarrow H^+$, $D^0 \rightarrow D^+$, $^3He^0 \rightarrow {}^3He^{++}$) the dependence of the energy and particle confinement on the plasma ion species in JET has been determined[7]. The measured particle confinement in deuterium L-mode discharges is found to be ~ 50% higher than in similar discharges in hydrogen (see Fig. 1(a)). The associated difference in the convective contribution to the energy loss is sufficient to account for the 15%-20% higher global energy confinement of deuterium compared to hydrogen plasmas (Fig. 1(b)). Calculations of the local thermal conductivity shown in Fig. 2, show essentially no dependence on ionic mass.

2.2 Simulated transport of thermalised α-particles

The injection of energetic beams of ^4He into deuterium plasmas in order to provide a known deposition profile in the core of the plasma allows the

outward transport of particles which are the equivalent of thermalised α-particles to be measured prior to the onset of helium recycling[8]. Following the injection of short pulse of He, the subsequent decay of the radial profile of He^{++} is measured using charge-exchange spectroscopy (which uses two of the D^0 heating beams as the CX source).

These experiments have been performed in both L- and H-mode regimes on JET and preliminary work has been done to compare sawtoothing and sawtooth-free phases. The results indicate a helium diffusion coefficient within the central half-radius of the plasma which varies from $0.3 \pm 0.1 m^2 s^{-1}$ (sawtooth-free L-mode)[9] to $0.6 \pm 0.1 m^2 s^{-1}$ (sawtoothing H-mode)[8]. In all regimes thermal He^{++} is effectively removed from the core and relationship between He^{++} confinement time (τ_{He}) and energy confinement time (τ_E) of

$$\tau_{He}\ (\text{core})/\tau_E\ (\text{core}) \leq 3$$

can be inferred. This compares favourably with the condition required[10] for prevention of ignition quench by helium-ash accumulation in a particular region of the plasma, and indicates that core ignition could be maintained in a reactor plasma against α-particle build up.

2.3 High β_T plasmas

NBI has enabled high-β_T plasmas to be studied using H-mode confinement obtained in two regimes[11]:

a) Low toroidal field (≤1.4T) with plasma currents of 1.5 and 2MA.

b) Hot Ion (HI) H-modes with 3MA plasma current and toroidal field in the range 1.8-3.1T.

The JET database for high β_T plasmas is shown in Fig. 3 where the maximum β_T obtained is plotted against the Troyon limit prediction[12] ($\beta_T^{LIM} = 2.8I/aB_T$ with I in MA; a in m and B_T in Tesla). The best low B_T H-modes can be seen to exceed this limit by ~ 20% before a collapse phase

sets in. Low B_T discharges which limit below the Troyon limit always show Edge Localised Mode (ELM) activity. At the point at which the pressure limits, the growing n=1 and n=3 MHD activity in the plasma collapses suddenly and is replaced by strong n=2 activity. It has proved possible to exceed the Troyon limit at low B_T both in H-modes where $T_i \sim T_e$ and in 'hot ion' type discharges where $T_i > 1.5T_e$ (T_i/T_e up to 3 has been achieved). Both types of discharge show the effects of confinement degradation close at the β-limit, having confinement which is typically 1.7-1.9 greater than that given by Goldston L-mode scaling for the $T_i \sim T_e$ discharges. This compares with the more normal 2-2.2 enhancement factor for JET H-modes far from the β-limit. Theoretical predictions and experimental measurements[11] show that the discharges with the highest normalised β ($\beta_N = \beta_T/(I/aB_T)$) exceed the ideal ballooning limit in the centre of the plasma. The HI H-modes, which are covered in more detail below, limit at around $\beta_T \sim 0.85\ \beta_T^{LIM}$ ($\beta_N \sim 2.4$). The termination phase of these discharges is discussed in section 3.2. The thermal confinement of a group of these 3MA discharges with varying toroidal field and $\beta_N \geq 2$, shows a much stronger variation with toroidal field ($\sim B_T^{0.7}$) than the dataset of medium density H-modes where the exponent for B_T scaling is, within errors, equal to that derived from the ITER 92 H-P database ($\tau_E \propto B_T^{0.2}$)[13].

3. HIGH FUSION PERFORMANCE PLASMAS

The very high values of fusion performance in deuterium (D-D) plasmas achieved on JET are obtained in two modes known as the Pellet Enhanced Plasma (PEP) H-mode and the HI H-mode. Of these two modes the HI H-mode has achieved high fusion yields more reliably and more frequently and as a result was used for the FTE on JET[3].

The two modes represent the opposing approaches of creating a dense plasma core and heating it (PEP H-mode) or centrally-heating a low density plasma core and allowing the density to build up (HI H-mode).

3.1 PEP H-modes

In the PEP H-mode, the good confinement properties of the H-mode are combined with a peaked central density profile produced by pellet fuelling. The mode has been achieved with combined ICRF and NBI heating[14,15] and with NBI and ICRF heating separately in double null X-point plasmas in the range 3-3.6MA plasma current. The confinement inside the peaked profile region is found to be enhanced[15] over normal H-modes and this is possibly as a result of the negative shear which exists transiently (for periods ~1s) in this region[16]. This negative shear is a result of the generation of a large off-axis bootstrap current density (~1MA m^{-2}) which arises from the strong off-axis pressure gradient at the edge of the PEP 'core' of the plasma. As the current profile evolves, a number of MHD instabilities arise[16,17] and cause the deterioration of this enhanced mode of operation after a period ~1-1.5s. The longer duration and the highest fusion performance PEP H-modes are obtained with NBI plus a small amount of ICRF power. The highest fusion yield PEP H-mode achieved a peak neutron rate of $2{\cdot}1\ 10^{16} s^{-1}$ with 10·6MW of NBI and ~2MW ICRF power. The plasma at peak performance had very similar electron and ion temperatures ($T_i(0)$ = 9.8keV and $T_e(0)$ = 8.3keV) with a central deuterium density of ($n_D(0)$) $6{\cdot}5\ 10^{19} m^{-3}$ and an energy confinement time of $\tau_E = 0{\cdot}73$s. This gave a fusion triple product of $4{\cdot}7\ 10^{20} m^{-3}$skeV. The beam-plasma and thermal neutron rates were approximately equal.

The confinement properties of the PEP H-mode plasma can be clearly demonstrated with the application of pure NBI heating even though the

heating profile shows modest central power deposition. Fig. 4 shows the development of two NBI-heated discharges, one with a 4mm pellet injected at 5 secs which shows the PEP density enhancement (Fig.5(a)) and the other with no pellet. The two discharges have identical (11·0MW) NBI heating but it can be seen that the PEP discharge achieves superior stored energy and, eventually, superior temperature values compared to the normal H-mode discharge. A transport analysis with the TRANSP code shows that the energy deposited in the core of the PEP discharge is only ~25% higher than the H-mode shot, nevertheless the same temperature is obtained with three times the central density (Fig. 5(b)). The effective thermal diffusivity (χ_{eff}) as a function of normalised minor radius is shown for the PEP + H-mode and H-mode plasmas in Fig. 6. χ_{eff} is reduced by a factor 2 on the inner half of the minor radius for the PEP + H-mode. Also shown (shot 22624) is the highest fusion performance PEP H-mode described in ref.15. This shows a similar region of enhanced χ_{eff} is present irrespective of heating system mix. Work is in progress to relate this improved confinement more quantitatively to the density gradient and negative shear variation.

3.2 Hot Ion (HI) H-modes

The possibility of an energy efficient route to ignition via the hot ion regime has already been identified by previous workers[18]. This is determined by the fact that the minimum $n\tau_E$ product for ignition from the Lawson criterion occurs at ion temperatures in the 20-30keV range[19] and also because the α-particles produced should ultimately provide sufficient electron heating to achieve $T_i = T_e$, the conditions in a thermonuclear plasma in thermal equilibrium. Experimental experience on JET has shown that the starting point of low density has produced the highest fusion performance. The HI H-mode plasmas are produced using strong central NBI heating to initial low

density ($<n_e>$ ~1·5-2.0 $10^{19}m^{-3}$) target plasmas. They are characterised by $T_i \geq 1{\cdot}5\ T_e$ and density profiles which are moderately peaked ($n_e(0)/<n_e>$ ~1.5) The plasmas have low edge recycling and both power and particle deposition profiles from the beams are peaked at the plasma axis. The discharges where this mode is obtained are always in the X-point (magnetic separatrix limited) configuration. Both SNX and DNX HI H-mode plasmas have been produced. Those with the longest duration and the best purity have an X-point which is a significant distance (up to 0.2m) from the vessel target tiles. The central power and particle deposition, which peaks around $n_e(0)$ ~2 $10^{19}m^{-3}$, varies little (<30%) over the range 1-4 $10^{19}m^{-3}$ due to the mix of 80 and 140keV D^0 beams. This allows the density to build up in these HI H-modes without significant deterioration in the heating performance.

Bickerton et al.[20] have identified the twin important criteria for the hot ion mode with $T_i/T_e > 1{\cdot}5$. They are: the ability of the additional heating system to predominantly heat the ions directly and the necessity for the equipartition time (τ_{eq}) to be significantly longer than the global confinement time. These then define a 'hot ion' region of the $n_D(0){\cdot}T_i(0){\cdot}\tau_E$ vs $T_i(0)$ plane (in which the ignition criterion is usually plotted)[19] given by

$$n_D(0){\cdot}T_i(0){\cdot}\tau_E < 4{\cdot}57\ 10^{17}\ T_i^{5/2}(0)\ . \qquad (1)$$

This line is shown on Fig.11. It eventually intersects the ignition ($Q=\infty$) curve at $T_i(0)$~50keV and would clearly not be the optimum route for the whole process to ignition. The required ion temperature can be reduced, however, in regimes where the ***ion*** energy confinement substantially exceeds the ***electron*** energy confinement. This is achieved in the JET HI H-modes.

For deuterium, the critical energy for injection (E_c) at which the instantaneous power transfer to the plasma ions equals that to the electrons is given by $E_c \sim 19\ T_e$, which yields critical values of the electron temperature of ~ 4 and 7keV for the 80kV and 140kV beams respectively. Integration on the slowing down spectrum results in ~ 80% of the energy being transferred

to the ions even for injection at E_c. The JET D^0 beams preferentially heat the plasma ions for both injection energies given the range of electron temperatures routinely achieved in JET.

Figs. 7(a) and (b) show the variation of T_i and T_e as a function of the injected power per particle for plasmas in both the L and H-mode confinement regimes for a subset of JET plasmas. The highest values of ion temperature achieved in HI H-mode plasmas approach that to be expected from the thermalization of the injected beam particles in the absence of appreciable energy loss from the centre by thermal conduction. This indicates good energy confinement properties for the ions and local transport analysis of such discharges[21] shows that the central ion thermal conductivity is significantly better than $\chi_i \sim 0.4 m^2 s^{-1}$ for some HI H-mode plasmas compared to $\chi_i \sim 1.6 m^2 s^{-1}$ for L-mode discharges (see Fig. 7(c)). The ion thermal confinement is much better than the electron confinement in these discharges[21], although very good central electron confinement ($\chi_e \sim 0.5 m^2 s^{-1}$) is sometimes achieved.

This enhanced confinement leads to a separation of these HI H-mode discharges from the bulk of the JET H-mode database where $T_i \sim T_e$. This is shown in Fig. 8 where the thermal energy confinement in these discharges is plotted against the scaling derived for JET and DIII-D ELM-free H-modes[22]. This scaling was derived from medium power (5-10MW) H-modes from JET with density and q values similar to the HI H-modes. The HI H-modes differ from the dataset only in the power per particle values and in having a slightly more peaked density profile. The DIII-D 'VH-mode' discharges[23], are also indicated on Fig. 8. These discharges are thermal plasmas with $T_i \sim T_e$ but are similar to the JET HI H-modes in that they have a large fraction of the current (~30%) driven by the bootstrap mechanism at the plasma edge. The good confinement results in a strong pressure gradient at the plasma edge which elevates the bootstrap current and it is possible that this is leading to

further enhanced confinement. Also shown on Fig. 8 are other JET discharges in regimes where the bootstrap current is playing an important role. These include the PEP H-mode and low current (1-1.5MA) ICRF H-mode discharges at high q ($q_{95} \geq 10$) with current driven dominantly (~70%) by the bootstrap mechanism[24]. These other JET regimes, however, differ more strongly from the plasma parameters at which the scaling was determined, either by very different q values or density profiles.

The combination of high confinement and high ion temperature leads the HI H-modes to dominate the high Q_{DD} dataset for JET plasmas. This is illustrated in Fig. 9 where plasmas with additional heating power levels ≥10MW are shown. Some HI H-mode discharges have used small amounts (≤6MW) of ICRF power, tuned to the hydrogen minority, in an attempt to improve the fusion yield either by coupling to the deuterium beams at $2\omega_{cD}$ or to increase the beam slowing-down time by increasing electron temperature[25]. The first option would be unattractive in a D-T scenario since the deuterium energy 'tail' produced would rapidly reach an energy too high to make an effective contribution to D-T reactivity. The second is of marginal use in the present JET regimes where beam slowing down is still predominantly on the plasma ions. Thus although enhancements in the plasma reactivity have been achieved by the addition of small amounts of RF power[25], when normalised to obtain Q_{DD} they either lead to no enhancement or a slight degradation. In contrast, incremental ***beam*** power is more effective. The fusion rate in JET deuterium plasmas (R_{DD}) is approximately proportional to the square of the NBI power deposited in the centre of the plasma (see Fig. 10). This gives $Q_{DD} \propto P_{NBI}(\text{central})$.

The enhanced ion confinement of the JET HI H-modes leads to the existence of hot ion discharges over a wider regime than given simply by the application of equation (1). This is shown in Fig. 11. The discharges with the highest fusion triple product (up to 9.0 $10^{20} m^{-3} s$ keV) are all medium density

($\langle n_e \rangle \sim 3.75\ 10^{19} m^{-3}$, $n_e(0) \sim 5\ 10^{19} m^{-3}$) at the termination of the high performance phase and in the absence of termination would approach conditions where $T_i \sim T_e$. This puts them in a more optimal regime on the route to ignition.

The enhanced confinement phase of the HI H-modes is a transient regime, lasting up to ~1.7s with the loss power, $P_{LOSS} = (P_{in} - \dot{W})$ being <70% of the input power (P_{in}) in most cases. The termination of the high performance phase is accompanied by a sharp influx of carbon impurities from the machine X-point target tiles, but it is thought that this is a consequence of, rather than a cause of, the termination phase. In this respect it is different from the 'carbon-bloom' events which have previously limited JET performance in medium-power H-modes[26], and which were the result of tile overheating and enhanced carbon emission in the divertor region. These termination events are characterised by a roll-over or dramatic collapse of the plasma stored energy and neutron yield (the 'X' event) but are variable in circumstance, sometimes being accompanied by a giant ELM and sometimes by a sawtooth coupling to an ELM on a very fast (100s of microseconds) timescale[3]. It is now thought[27] that MHD activity is responsible for most of the collapses seen in the high performance plasmas, but the exact nature of the modes (e.g. internal n=1 kink or resistive ballooning modes) is still under investigation. As mentioned in section 2.3, the best discharges reach normalised toroidal β's around 85% of the Troyon limit. The β_T achieved depends inversely on the purity of the plasma.

The evolution of the neutron yield for one of the best fusion plasmas (pulse 26087 with $I_p = 3.1MA$ and $B_T = 2.8T$) is shown in Fig. 12 compared to a simulation of the TRANSP code. It can be seen that the thermal plasma yield is 60% and rising at the X event.

4. THE FIRST TRITIUM EXPERIMENT (FTE) ON JET

The highly reliable performance of the NBI system and the crucial role of high power NBI heating in the achievement of high fusion performance made the NBI-heated HI H-mode highly suitable for the FTE with D-T plasmas in JET. The main objectives of this experiment have been listed in ref. 3 and included the production of >1MW of fusion power in a controlled way: the validation of transport codes as a basis for accurately predicting D-T plasma behaviour from results obtained in D-D plasmas; the determination of tritium retention properties and discharge cleaning techniques; the demonstration of tritium usage technology and establishment of safe procedures for handling tritium.

In addition to the choice of the NBI-heated HI H-mode, it was decided to use JET PINIs to ***fuel*** the plasma with tritium. This choice was motivated by several factors: the limited amount of tritium to be used; the need to minimise the tritium contamination of the torus vessel first wall surfaces; the need to maximise the deposition of tritium atoms in the plasma centre and the requirements to test the operation of the heating and fuelling system 'offline' without a target plasma. The first two factors were related to the requirement to avoid delays in the shutdown of JET for the upgrade to the Pumped Divertor program[28] either arising from vessel activation or vessel tritium inventory being too high.

To maximise the ***particle*** fuelling of tritium from each PINI, the '80kV' version of the PINI[1] was used for tritium injection. This gives a higher extracted current and neutralisation efficiency than the '140kV' version. A more gas-efficient percentage of neutrals is thus delivered to the torus. The computed particle fuelling in the plasma centre for D^0 and T^0 beams is shown for various plasma densities in Fig. 13 for the PINI types used in the FTE (the FTE configuration is listed in table 1). It may be seen that the variations in deuterium and tritium central fuelling are reasonably well matched over the HI H-mode range ($<n_e> = 1.5 - 4\ 10^{19} m^{-3}$).

The total inventory of tritium available for the FTE was 0.2gm (2000Ci or 74TBq). The tritium neutral injection characteristics for one PINI are shown in table

2, where it can be seen that the tritium gas required for a 2s injected pulse is only 0.012gm per PINI. This very economical performance was achieved after an extensive test bed program[29] of ion source and gas feed modification to the PINIs. Nevertheless, sufficient tritium was only available for a very limited number of pulses, dictating a highly reliable performance from the injectors, and a small number of shots to change from deuterium to tritium in the PINIs. This changeover period was optimised in tests changing from hydrogen to deuterium gas[29] and was accomplished by running several gas-free filament degassing pulses in the PINI ion sources. The tritium gas was supplied to the PINIs from a heated uranium storage bed (U-bed). The technical details of the development of this U-bed gas system are given in ref. 30.

4.1 Measurements of tritium diffusion: the '1% tritium' experiment

In order to test both the capabilities of the 14MeV neutron detectors, the transport prediction codes and the tritium handling and recovery systems[31] under very small inventory conditions, several discharges were performed with additional heating in which two of the PINIs were fed by a 1% tritium/99% deuterium mixture. These proved the satisfactory nature of the diagnostics and codes[3] and of the technology[31], but were also used to study the relative diffusion of deuterium and tritium. .

The similar deposition profiles of deuterium and tritium beam particles in the plasma had the consequence that, with continuous injection, it was not possible to use a transport code simulation to distinguish between widely differing assumptions about the relative diffusion of deuterium and tritium. This was overcome by using a 1% T_2 in D_2 feed to one PINI to provide a 1s pulse. The decay of the 14MeV neutron signal post-pulse was observed with space resolved detectors over a 0.6s period when the discharge was sawtooth-free. This has been compared to TRANSP code predictions where

different models for ***relative*** diffusion of tritium and deuterium were used. The 2.4MeV neutron emission from D-D reactions was found to be insensitive to the relative diffusion model[32] but the 14MeV emission profile did show some sensitivity, the differing models giving strongly differing tritium profiles during the decay. Fig. 15 shows the experimentally observed 14MeV neutron decay compared with TRANSP calculations for $D_T/D_D = 1$, 2 and 0.5. The results clearly indicate that the deuterium and tritium have similar properties and the transport of each isotope depends mainly on the local concentration gradient of that isotope. The diffusion coefficients are similar to those observed in other discharges, ie $0.3 m^2 s^{-1}$ in the centre of the discharge and around $2 m^2 s^{-1}$ at the edge.

4.2 The D-T fusion experiment

Before the full scale D-T fusion experiment, the parameters of the injectors were optimised in deuterium and then the change-over to tritium operation was achieved with only the filament degassing pulses mentioned above, followed by only 2 asynchronous pulses on the tritium PINIs in which 78kV beam pulses of 0.8s duration were extracted onto the beamline calorimeter. These first-ever tritium beams were obtained without breakdowns at the first attempt. They represent a major step-forward in the technology of NBI.

Two plasma shots with 14.3MW NBI power (including 1.5MW from the tritium beams) were then performed. These shots (described in more detail in ref. 3) were very similar, each producing a peak fusion power of about 1.7MW (a total fusion energy of about 2MJ), with peak neutron rate ~ $6\ 10^{17} s^{-1}$ (a total neutron yield of $7.2\ 10^{17}$ neutrons). The time history of the important plasma parameters of the second of these shots (pulse 26148) is shown in Fig. 15. At the end of the high power beam phase the tritium content of the discharge is

about 11%. It is clear that the period of high neutron emission is terminated after 1.3s of high power NBI by an event which falls into one of the classifications (sawtooth coupling to an ELM on a fast timescale) of the 'X' - events discussed in section 3.2. The normalised β reached at the termination (β_N ~ 1.9) is somewhat lower than the best pure D-D shot (in Fig. 12) which reaches β_N ~ 2.3, but is within the range of values achieved in HI H-mode shots. The lower value stems almost certainly from the higher Z_{eff} of the target plasma for pulse 26148 (Z_{eff} = 2.4) when compared to pulse 26087 (Z_{eff} = 1.7). The confinement enhancement for the FTE pulse 26148 is shown compared to the DIII-D/JET scaling in Fig. 8 where it clearly forms part of the enhanced dataset.

The termination phase of the D-T pulses does not appear to be related to the presence of tritium or a substantial population of α-particles. The toroidal β of the α-particles (β_α) reaches about 1.5 10^{-4} at the peak performance of the discharge according to a TRANSP code analysis[33]. For the relatively broad α-particle profile inferred from the code, the α pressure is significantly (factor 6) below the level at which Toroidal Alfvèn Eigenmode (TAE) instabilities would be expected to cause α-loss effects (see, e.g., ref. 34). The presence of α-particles in the plasma was detected by the reception of Ion Cyclotron Emission (ICE) from the α's using an ICRF antenna as a probe[35]. Up to the (X-event) termination of the high performance phase the ICE does not show any effects of strong collective α-particle loss. The plasma density at the X-event is high enough ($\langle n_e \rangle$ = 2.5 $10^{19} m^{-3}$) to give a ratio of the α-particle velocity to the Alfvèn velocity (V_α/V_A) of around 1.5, a value at which TAE modes are more stable than at V_α/V_A ~ 1. The development of the HI H-modes towards high densities (as in pulse 26087 with $\langle n_e \rangle$ ~ 3.5 $10^{19} m^{-3}$) should take future discharges further away from the maximally unstable point. The relatively broad birth profile of the α's produced in the HI H-mode,

especially when compared to the PEP-H mode, is also favourable in this respect.

The ratio of fusion power (P_{fus}) to input power (P_{in}) for the 2 D-T pulses was approximately 0.12. If the energies and powers in the injectors are kept the same as in the experiment and the plasma is assumed to be a 50:50 D-T mix then the fusion power output from pulse 26148 would increase from 1.7 to 4.6MW (43% thermally produced) and the ratio of P_{fus}/P_{in} would be 0.32. For the best D-D pulse (26087) an extrapolation to 50:50 D-T conditions would yield a fusion output of 9.6MW (60% thermally produced) with $P_{fus}/P_{in} = 0.64$. The fusion Q for a thermal D-T plasma (Q_{DT}^{th}) with the same plasma characteristics (n_e, T_e, Z_{eff}, $<n_e/n_e(0)$ etc) as these plasmas can be defined as

$$Q_{DT}^{th} = P_{fus}(thermal)/(P_{LOSS} - P_{\alpha}) .$$

On this basis the D-T pulse 26148 would have $Q_{DT}^{th} \simeq 0.22$ at its peak performance (for a 50:50 D-T mix) and the D-D pulse 26087 would extrapolate to $Q_{DT}^{th} \simeq 0.75$. These values are lower than the predicted steady state values shown in Fig. 11 (i.e. Q ~ 1 for pulse 26087 and Q ~ 0.45 for pulse 26148), because the energy confinement time used in establishing the fusion triple product includes the fast particle content of these JET plasmas which gives a contribution up to 25% of the diamagnetic stored energy. Ref. 36 discusses this in more detail.

4.3 Tritium decontamination and recovery from the NBI system

The total amount of tritium fed to the injectors in these experiments was 1003(±70)Ci (37TBq) and of this (54±6)Ci was injected into the torus and the neutral beam duct. After the experiments, tritium recovery was successfully attempted using both discharge cleaning regimes and plasma discharges in which careful measurements were made[37]. These measurements were

supplemented by analysis of tiles from the torus walls[38] and the total estimated residual inventory in the vessel is about 2Ci. Most of the torus wall could be classified as low level waste (0.3μ Ci.gm^{-1}) and the rest could be reduced to this level by outgassing at elevated temperatures[32].

The bulk of the tritium in the NBI injectors was pumped onto the cryopanels and was recovered safely ensuring regeneration with many useful procedures being validated for the final JET D-T phase[39]. A small amount, estimated as (70±5)Ci, was implanted in the injector calorimeter and ion dumps. This was desorbed using deuterium beams[40]. This desorption process required about 10^4 coulomb of integrated beam fluence onto the dump. The contamination of tritium on the dumps was estimated from the D-T neutron yield from the drive in d(t)→(α)n reaction, measured by a 14MeV neutron detector. The mechanisms for target depletion by drive-in beams are discussed further in ref. 40. The contamination remaining in the injectors is no longer a problem.

5. SUMMARY AND CONCLUSIONS

The JET NBI system has contributed widely to the progress of the fusion physics program both as a general method of attaining high performance plasmas and in experiments which utilise the specific heating and fuelling qualities of the beams. Amongst the latter type of experiments the approximate independence of energy confinement on plasma isotope mass and the information on helium and tritium diffusion coefficients are important results. NBI heating has allowed the study of plasmas close to the β limit over a wide range of conditions: in high performance plasmas it has been possible to establish results on enhanced confinement regimes close to the β limit (where global energy confinement shows a strong toroidal field scaling); in high density plasmas where confinement enhancement of around a factor 2 is seen in the PEP enhanced core of an H-mode

and in HI H-modes where the energy transport in the plasma ions attains low values $\leq 0.4 m^2 s^{-1}$. These discharges show global thermal energy confinement which is enhanced over normal H-modes by a factor 1.6-2.0.

The HI H-mode has been developed to medium density regimes where $n_e(0)$ is around $5\ 10^{19} m^{-3}$. These plasmas take the HI regime to more favourable regions of the fusion triple product diagram and should re-open the study of the HI H-mode as a route to ignition. The best JET HI H-modes have a fusion triple product $(n_D(0)T_i(0)\tau_E)$ of ~ $9.0\ 10^{20}(\pm 1\ 10^{20})\ m^3\ keV\ s^{-1}$.

The use of tritium beams to create high fusion power (>1MW) in a deuterium-tritium plasma for the first time was an extremely successful exercise with many useful lessons being learned for the active (D-T) phase of JET. The fusion yield of the plasmas obtained was around 12% and the α-particle β came within a factor of 6 of the predicted limit for TAE instabilities, none of which were observed.

The NBI configuration for the final D-T phase of JET (in 1995-6) will have 12.4MW of 160kV T^0 beams and 7.6MW of 140kV D^0 beams. The results of the HI H-mode development on JET show Q_{DD} scaling with input NBI power. This indicates that, provided the best performance plasma parameters can be reproduced in the D-T conditions, a D-T fusion yield of Q_{DT} ~ 1 will be achievable in JET. At this level, significant α-particle physics will certainly be possible and there is an indication that the development of the HI H-mode to higher densities might offer the choice of testing or avoiding TAE instabilities.

Acknowledgements

The main authors have great pleasure in acknowledging the contributions of the whole JET Team to this work and particularly pay tribute to the continuing commitment and dedication of their colleagues in the Neutral Beam Heating Division of JET. Stimulating and useful discussions with Drs. B. Balet, C.D. Challis, J.G. Cordey, A. Gibson, T.T.C. Jones, P. Smeulders and K. Thomsen are also gratefully acknowledged.

References

1 G. Duesing, H. Altmann, H. Falter, A. Goede, R. Haange, R.S. Hemsworth, P. Kupschus, D. Stork and E. Thompson, Fusion Technology 11, 163 (1987).

2 H.P.L. de Esch, P. Massmann, A.J. Bickley, C.D. Challis, G.H. Deschamps, H.D Falter, R.S. Hemsworth, T.T.C. Jones, D. Stork, L. Svensson and D. Young in Proceedings of 14th Symposium on Fusion Engineering (IEEE, New York, 1992), vol. 1, p.86.

3 The JET Team, Nucl. Fusion 32, 187 (1992).

4 C.D. Challis, A.J. Bickley, A. Browne, H.P.L. de Esch, M. Fogg, T.T.C. Jones, D. Stork and L. Svensson, in ref. 2, p.62.

5 P.J. Lomas and the JET Team in Plasma Physics and Controlled Fusion Research, Würzburg, Germany, 1992 (IAEA, Vienna, in press).

6 T.T.C. Jones, B. Balet, M. Brusati, M. Bures, M. Hugon, K.D. Lawson, P.J. Lomas, P.D. Morgan, H.W. Morsi, P. Nielsen, G. Sadler, R. Sartori, D.F.H. Start, D.D.R. Summers, A. Tanga, A. Taroni, K. Thomsen and D.J. Ward in Proceedings of the 1992 International Conference on Plasma Physics, Innsbruck 1992 (Europhys. Conf. Abstracts, 16C(I), 3 (1992).

7 J.G. Cordey and the JET Team, in ref. 5.

8 T.T.C. Jones, M.G. von Hellermann, A.J. Bickley, D. Boucher, P. Breger, C.D. Challis, J.P. Christiansen, G.A. Cottrell, J.F. Davies, H.P.L. de Esch, M. Fogg, J. Frieling, F.B. Marcus, P.D. Morgan, H. Morsi, R. Prentice, G. Sadler, M.F. Stamp, D. Stork, H.P. Summers, L. Svensson, A. Tanga, A. Taroni, P.R. Thomas, E. Thompson and R. Wolf in Proceedings of the 18th European Conf. on Contr. Fus. and Plasma Phys., Berlin 1991 (Europhys. Conf. Abstracts 15C (i), 185 (1991)

9 L.D. Horton, B. Denne-Hinnov, A. Gondhalekar, L. Lauro-Taroni, T.T.C. Jones and M. von Hellermann, in ref. 5.

10 F. Reiter, G. Wolf and H. Kever, Nucl. Fusion 30, 2141 (1990).

11 D. Stork, B. Alper, S. Ali-Arshad, H.J. de Blank, H.P.L. de Esch, A. Edwards, T.C. Hender, R. Keonig, G.J. Kramer, F.B. Marcus, M.F. Nave, D.P. O'Brien, J. O'Rourke, P. Smeulders, M.F. Stamp, F. Tibone, B.J.D. Tubbing, A. Zolfaghari and W. Zwingmann in ref. 6, p.339.

12 F.S. Troyon, R. Gruber, H. Sauremann, S. Semenzato and S. Succi, Plasma Phys. and Contr. Fusion 26, 209 (1984).

13 O. Kardaun, F. Ryter, U. Stroth, A. Kus, J.C. de Boo, D.P. Schissel, G. Bramson, T.N. Carlstrom, K. Thomsen, D.J. Campbell, J.P. Christiansen, Y. Miura, N. Suzuki, M. Mori, T. Matsuda, H Tamai, T. Takizuka, S. Itoh and K. Itoh in ref. 5.

14 B.J.D. Tubbing, B. Balet, D.V. Bartlett et al., Nucl.Fusion 31, 839 (1991).

15 M. Keilhacker and the JET Team, Plasma Phys. and Contr.Fusion 33, 1453 (1991).

16 M. Hugon, B.P. van Milligan, P. Smeulders et al., Nucl. Fusion 32, 33 (1992).

17 P. Smeulders, A. Edwards, G. Fishpool, T.C. Hender, M. Hugon, B. van Milligan, C. Nardone, G. Neill, L. Porte, S. Wolfe, W. Zwingmann in ref.8, Vol.II, p.53.

18. M.L.Watkins, T.E. Stringer, A. Gibson, W.G.F. Core, I.L. Robertson, J.G. Cordey and J.J. Field in Plasma Physics and Controlled Fusion 1980 (IAEA, Vienna, 1981).

19. J. Wesson, Tokamaks (Oxford Science Publications, Oxford 1987), pp.8-9 and references therein.

20 R.J. Bickerton and the JET Team, Plasma Phys. and Contr. Fusion 29, 1219 (1987).

21 H.P.L. de Esch, F. Tibone, B. Balet, A.J. Bickley, C.D. Challis, J.G. Cordey, T.T.C. Jones, D. Stork and M. von Hellerman in ref. 8, p.189.

22 D.P. Schissel, J.C. de Boo, K.H. Burrell, J.R. Ferron, R.J. Groebner, H. St. John, R.D. Stambaugh, B.J.D. Tubbing, K. Thomsen, J.G. Cordey,

M. Keilhacker, D. Stork, P.E. Stott and A. Tanga, Nucl. Fusion 31, 73 (1991).

23 T.C. Simonen and the DIII-D team in ref. 5.

24 C.D. Challis et al., submitted to Nuclear Fusion.

25 M. Bures, B. Balet, D. Campbell, G.A. Cottrell, T. Elevant, L-G. Eriksson, J. Jacquinot, N. Jarvis, T. Jones, R. Konig, P. Lomas, F. Marcus, E. Righi, G. Sadler, D.F.H. Start, A. Tanga, P. van Belle and M. von Hellermann in ref. 6, vol.II, p.881.

26 D. Stork, D.J. Campbell, S. Clement N. Gottardi, L. de Kock, C.G. Lowry, P.D. Morgan, R. Reichle, G. Saibene, P. Smeulders, D.D.R. Summers and P.R. Thomas in ref. 8, p.357.

27. G. Janeschitz and the JET Team, in ref. 5.

28 P.H. Rebut and the JET Team, in Plasma Physics and Controlled Nuclear Fusion Research, Washington, 1990 (IAEA Vienna, 1991), vol. 1, p.27.

29 P. Massmann, H.D. Falter, A.J. Bickley, G.H. Deschamps, D. Hurford and E. Thompson, in Proceedings of 17th Symposium on Fusion Technology, Rome, 1992 (North Holland, Amsterdam, in press).

30 L. Svensson, D. Martin, A. Browne, D. Cooper, J.F. Davies, H.D. Falter, T.T.C. Jones and E. Thompson in ref. 29.

31 M. Huguet , A.C. Bell, S.J. Booth, C. Caldwell-Nichols, A. Çarmichael, P. Chuilon, N. Davies, K.J. Dietz, F. Delvart, F. Erhorn, H. Falter, B.J. Green, B. Grieveson, R. Haange, A. Haigh, J.L. Hemmerich, D. Holland, J. How, T.T.C. Jones, R. Laesser, M. Laveyry,J. Lupo, A. Miller, P. Milverton, G. Newbert, J. Orchard, A. Peacock, R. Russ, G. Saibene, R. Sartori, L. Serio, R. Stagg, S.L. Svensson, E. Thompson, P. Trevalion, E. Usselmann, T. Winkel and M.E.P. Wykes, Fusion Engineering and Design,19, 121 (1992).

32 A. Gibson and the JET Team, in ref. 5.

33 B. Balet, P.M. Stubberfield, J.G. Cordey, N. Deliyanakis, T.T.C. Jones, R. Konig, F.B. Marcus, D.P. O'Brien, G. Sadler, K. Thomsen and M. von Hellermann, submitted for publication in Nuclear Fusion.

34 C.Z. Cheng, R.B. White, G.Y. Fu, L. Chen, D.J. Sigmar, C.T. Hsu, A. Beklemishev, H.L. Berk, B. Breizman, S.C. Guo, Z. Guo, D. Lindberg and J.W. Van Dam in ref. 28 vol. 2, p.209.

35 G.A. Cottrell, V.P. Bhatnagar, O. da Costa, R.O. Dendy, A. Edwards, J. Jacquinot, M.F.F. Nave, A. Sibley, P. Smeulders and D.F.H. Start, accepted for publication in Plasma Physics and Contr. Fus. (1992).

36 A. Gibson and the JET Team, Plasma Phys. and Contr. Fus. 32 (11), 1083 (1990).

37 G. Saibene, R. Sartori, P. Andrew, J. How, Q. King and A.T. Peacock in ref. 31, p.133.

38 A.T. Peacock in ref. 29.

39 W. Obert et al., in ref 29.

40 H.D. Falter, E. Thompson, D. Ćirić, H.P.L. de Esch, Proceedings 10th Int. Conf. on Plasma Surface Interactions, Monterey 1992. (To be published in Journal of Nuclear Materials, in press).

Table 1: Injected Beam Power into JET

Atomic Species	Configuration (No. of PINIs x Voltage)	Injected Power (MW)
Hydrogen (H^0)	10 x 110kV + 4 x 80kV	7.0
Deuterium (D^0)	16 x 80kV 16 x 140kV 8 x 140kV + 8 x 85kV	21.6 15.0 23.0[a]
Tritium (T^0)	2 x 78kV	1.5
	Total FTE[b] 12 x 140kV D^0 2 x 85kV D^0 2 x 78kV T^0	14.3
^3He	16 x 140-150kV	13.0
^4He	8 x 120kV[c]	6.7

[a] Predicted. Configuration to be used in 1993-4 experiments.
[b] First Tritium Experiment.
[c] Operation limited to 120kV by deflection magnet.

Table 2: Tritium Neutral Beam Injection Characteristics for one PINI

Acceleration Voltage	78kV
Injected neutral specied mix: 78kV 39kV 26kV	power fraction: 79% 12% 9%
Equivalent atomic current	12A
Power Injected	0.75MW
Tritium gas requirement for 2s injected pulse	45mbl (ie 120Ci or 0.012g)

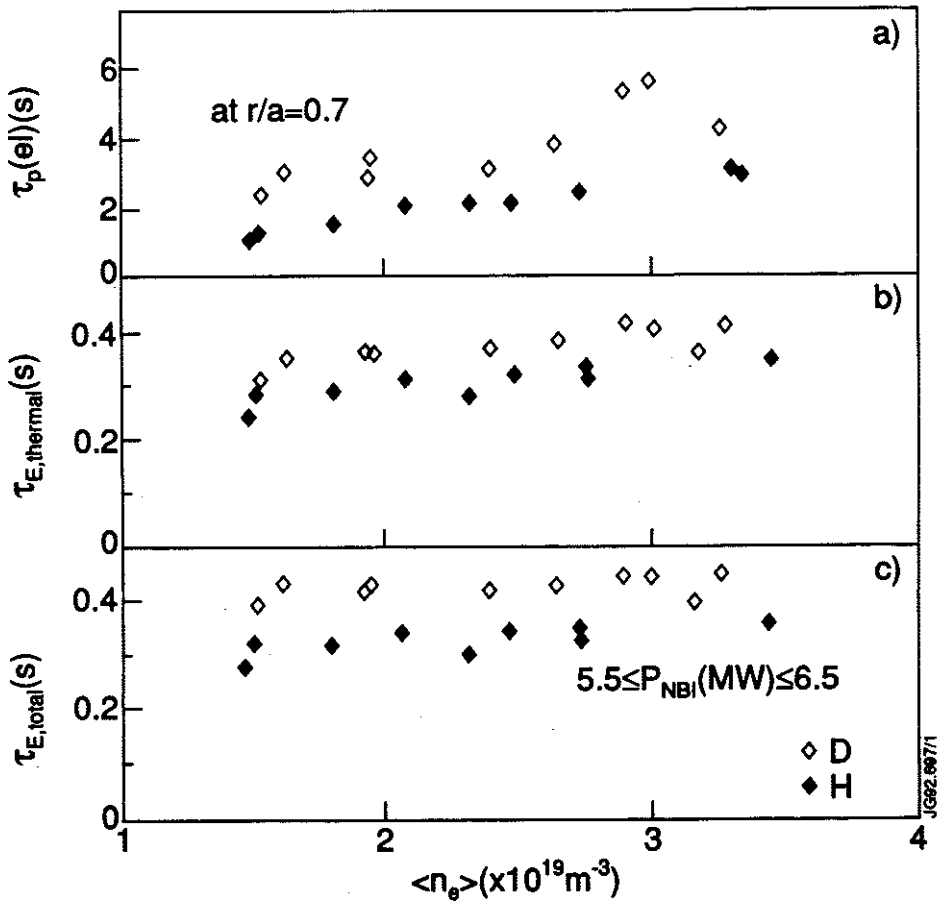

Fig. 1 *Confinement for JET H and D L-mode plasmas with heating by same NBI isotope.*

(a) *Particle confinement time vs density*

(b) *Thermal energy confinement. time vs density*

(c) *Total energy confinement time (thermal and fast) vs density*

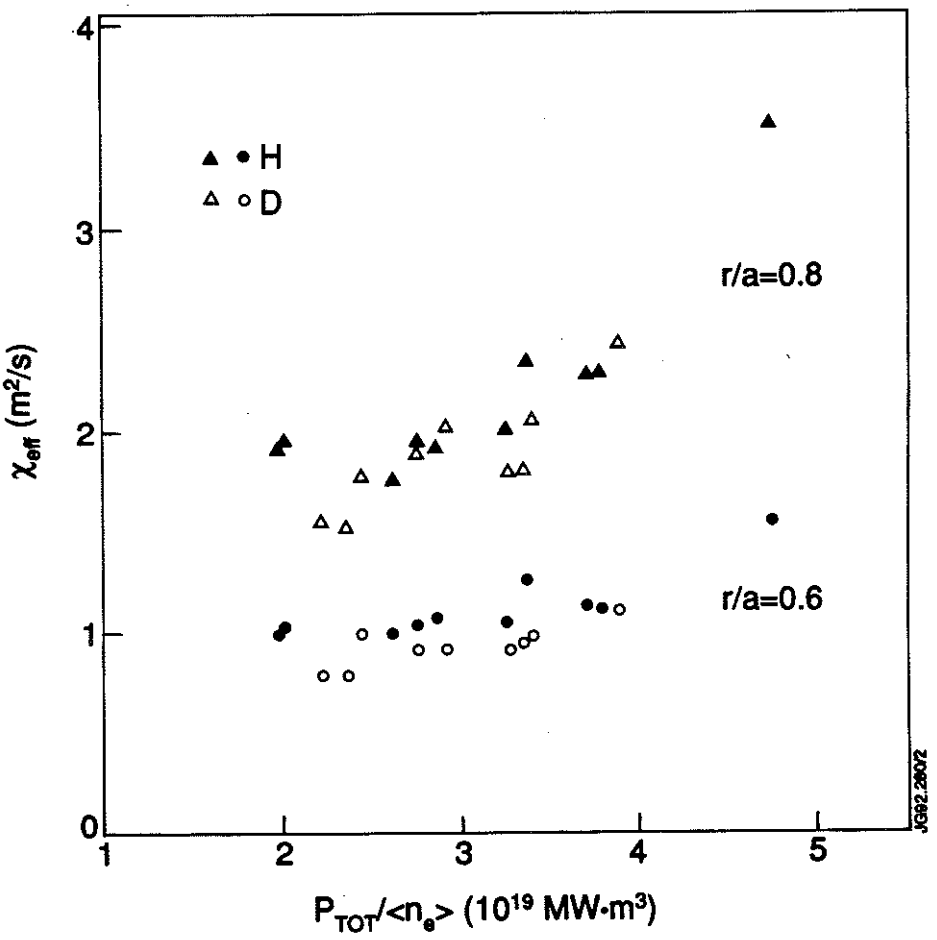

Fig. 2 *Single fluid thermal conductivity defined as*

$$\chi_{eff} = -\left(q_{tot} - \frac{3}{2}\Gamma_{tot}T_e\right) / \left(n_e + n_i\right)\nabla T_e$$

plotted as a function of average power input per particle for two different radial positions for the NBI heated H and D plasmas of figure 1.

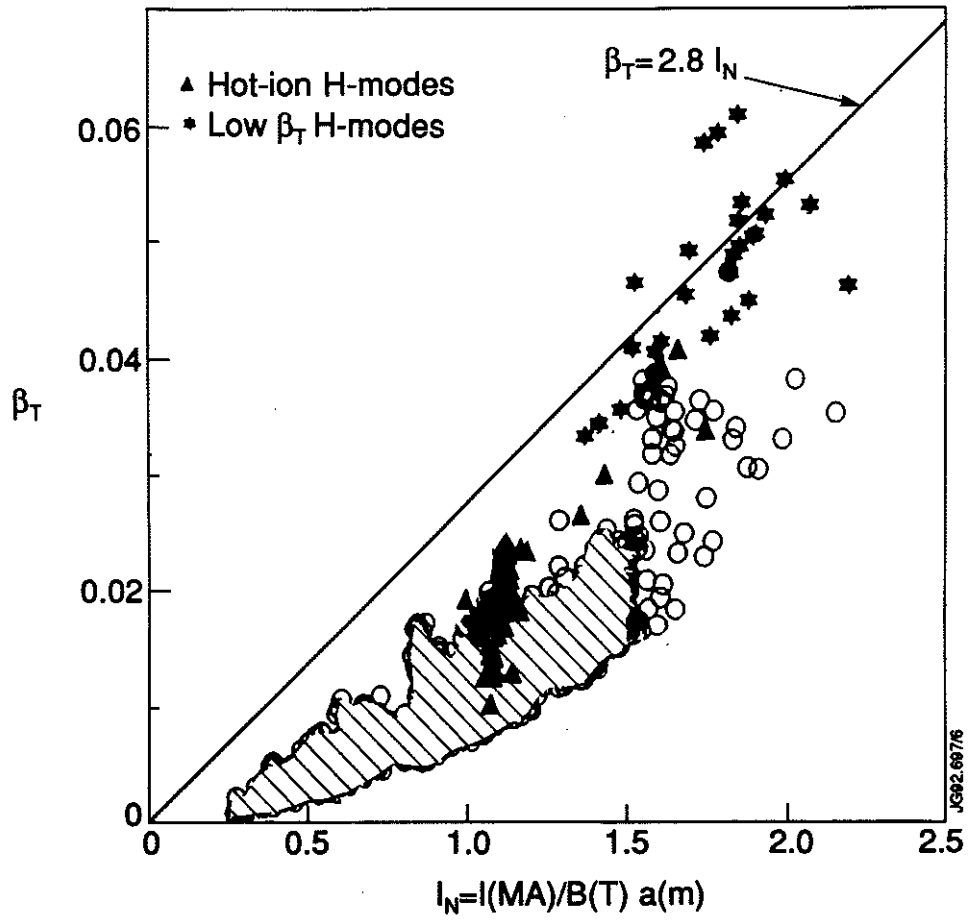

Fig. 3 *Maximum values of toroidal β (β_T) obtained for JET plasmas plotted against normalised plasma current I_N (defined as I_p/aB_T). The Troyon limit line (ref. 12) is shown. General points from the dataset are indicated by open circles (the cross hatched area indicates the bulk of this dataset). Hot Ion (HI) H modes are indicated by triangles and plasmas obtained with pure NBI heating at low toroidal field are indicated by stars.*

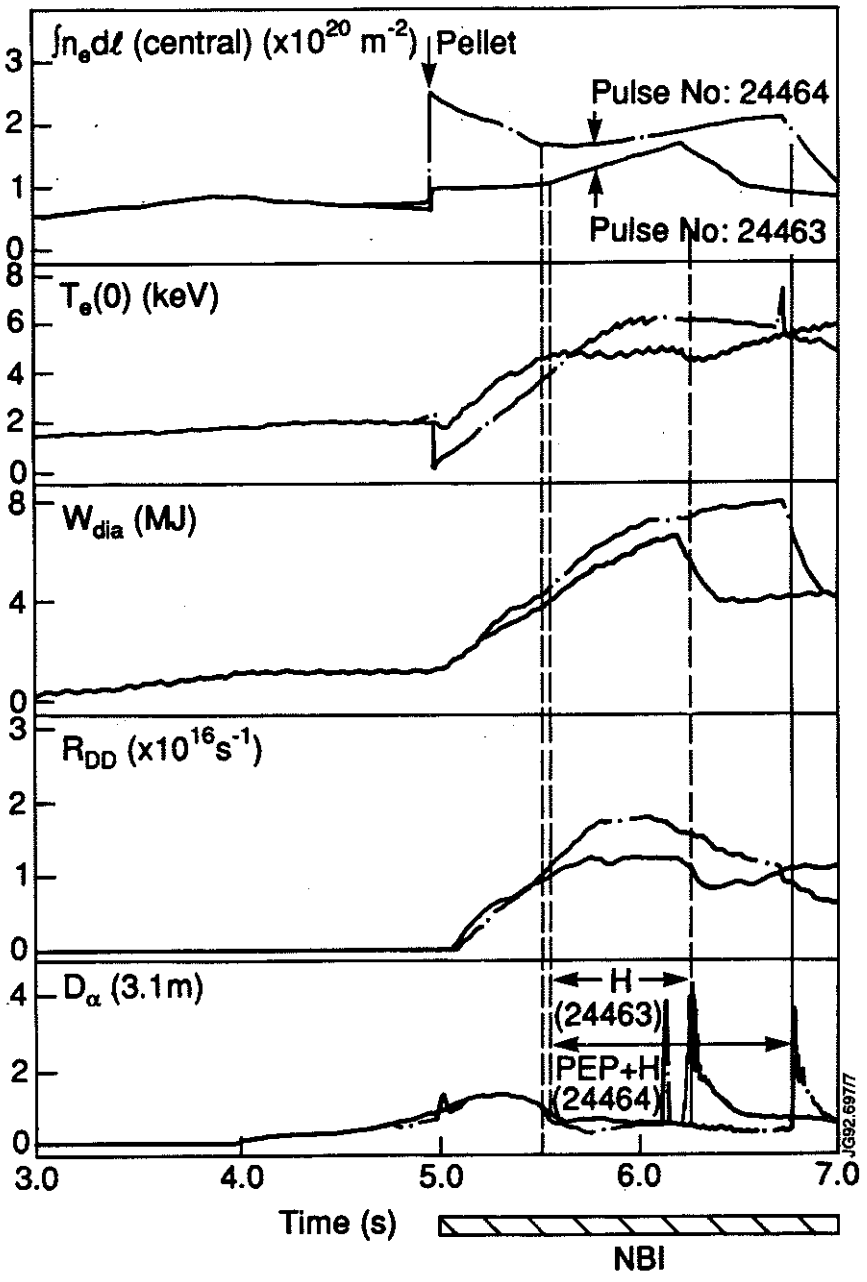

Fig. 4 *Comparison of time evolution of an NBI heated H-mode with (pulse 24464) and without (pulse 24463) the PEP density enhancement.*

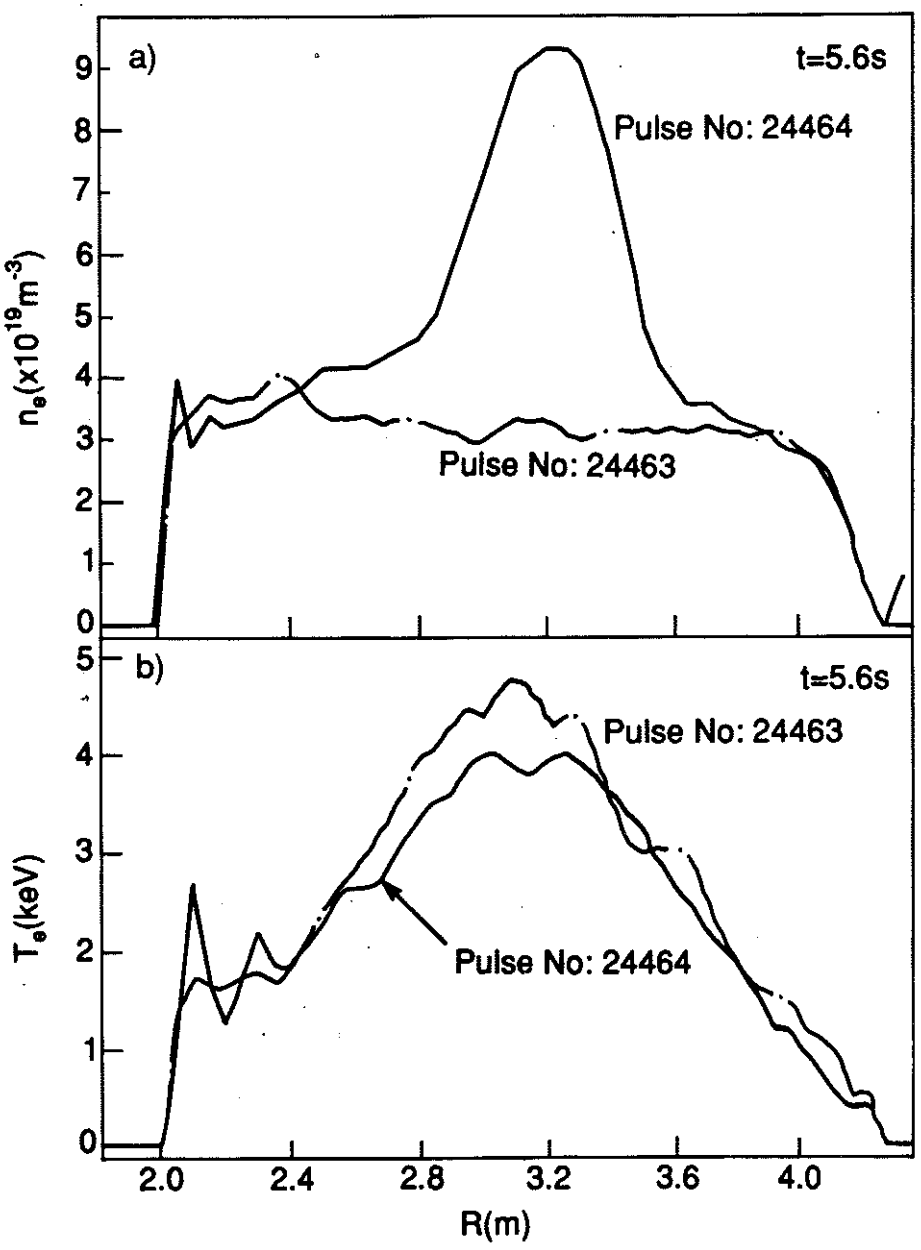

Fig. 5 *Profile comparisons for the 2 pulses in fig. 4. (a) Electron Density (b) Electron temperature. Data is derived from the LIDAR diagnostic. The PEP density enhancement can be clearly seen in pulse 24464.*

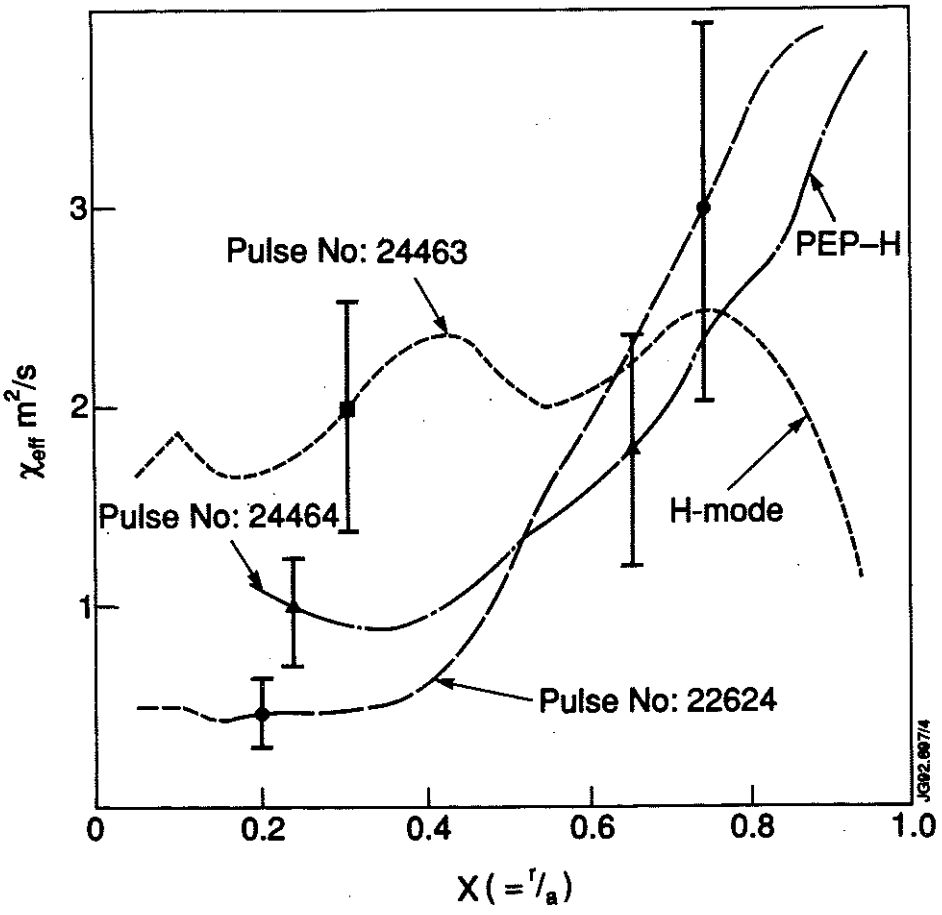

Fig. 6 *Local transport analysis results for the single fluid thermal conductivity (χ_{eff}) as a function of normalised minor radius (x) for the NBI H-modes with and without the PEP density enhancement. Also shown is the equilvalent analysis for the record fusion yield PEP H-mode (pulse No. 22624). Indicative error bars for χ_{eff} (~ ± 30%) are shown.*

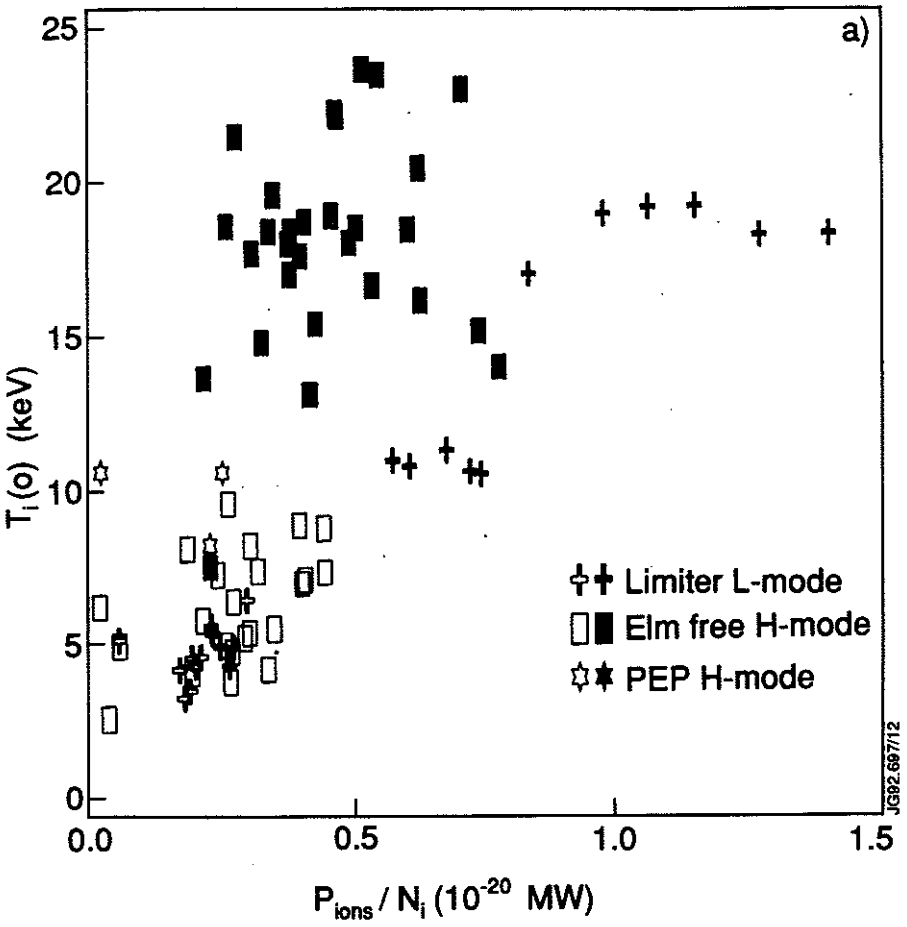
a)
25
20
15
10
5
0
T_i(o) (keV)
0.0
0.5
1.0
1.5
P_{ions} / N_i (10^{-20} MW)
Limiter L-mode
Elm free H-mode
PEP H-mode
JG92.697/12

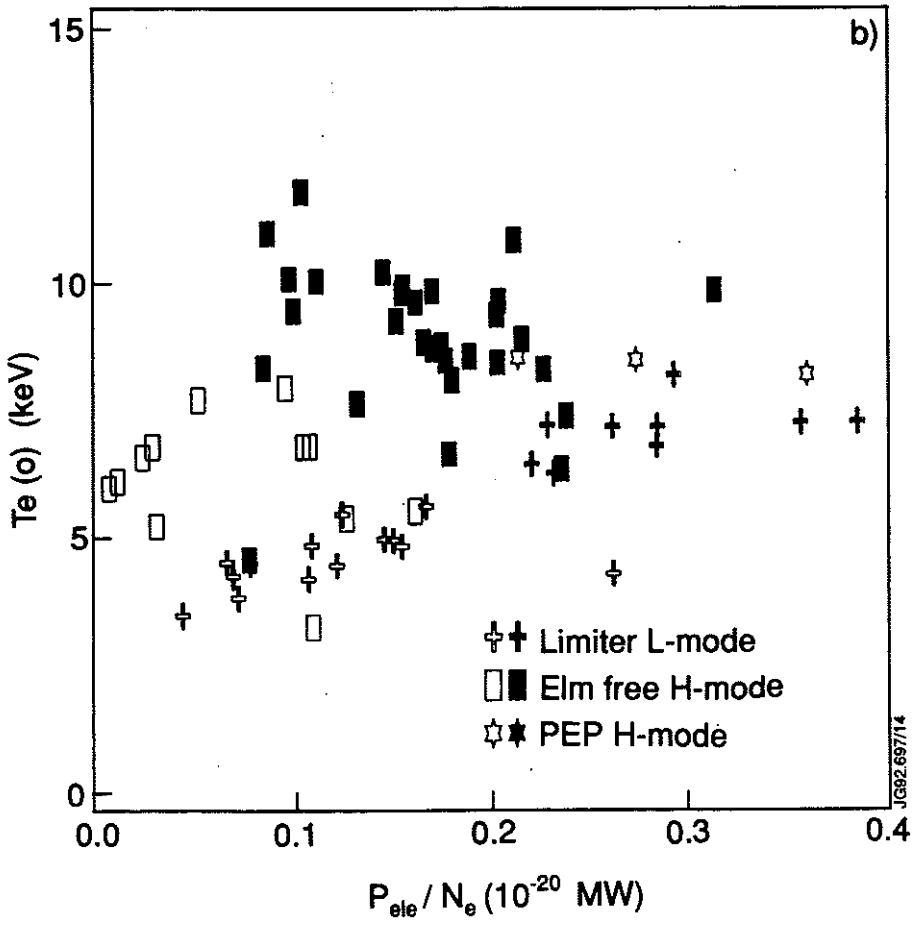
b)
15
10
5
0
Te (o) (keV)
0.0
0.1
0.2
0.3
0.4
P_{ele} / N_e (10^{-20} MW)
Limiter L-mode
Elm free H-mode
PEP H-mode
JG92.697/14

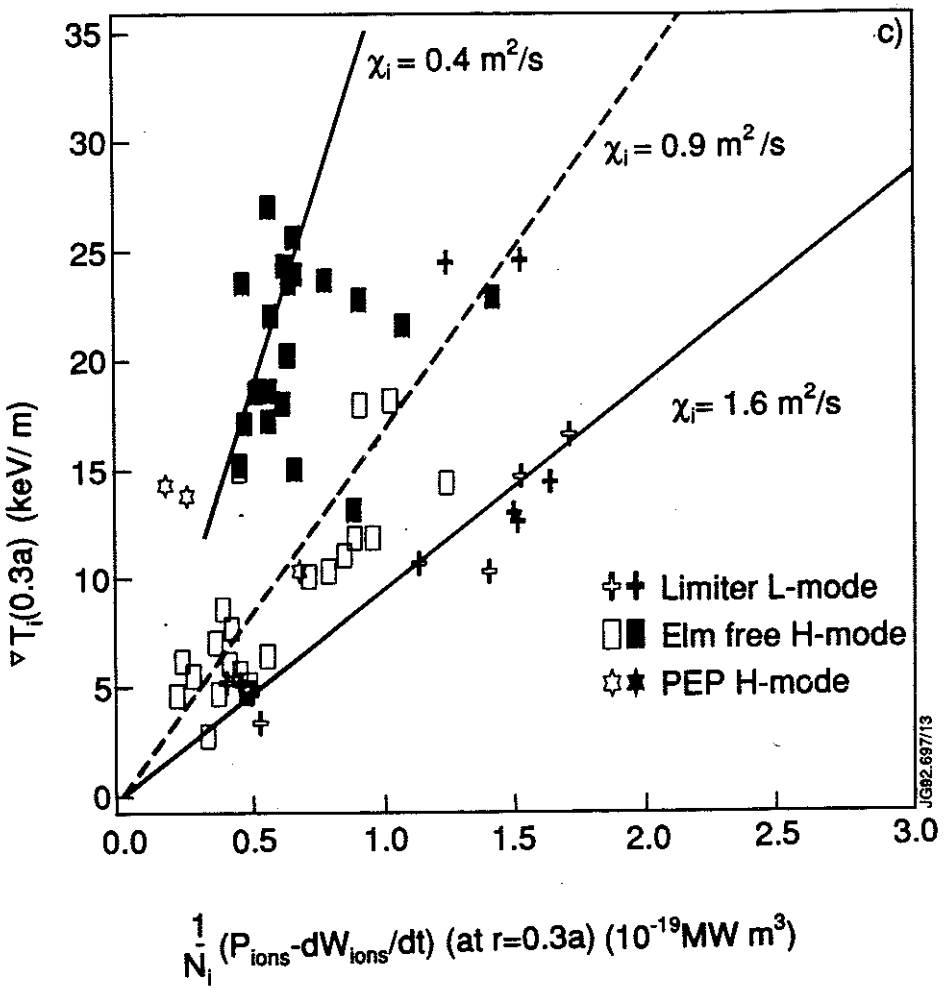

Fig. 7 *Heating and transport results for JET NBI heated plasmas with I_p = 3 MA, B_T > 2.2T and Z_{eff} < 3.2.*

The filled symbols represent hot-ion plasmas with T_i > 1.5 T_e.

(a) *Central ion temperature as a function of power delivered per ion.*

(b) *Central electron temperature as a function of power delivered per electron.*

(c) *Ion temperature gradient at r/a = 0.3 as a function of loss power per ion. The lines are labelled with the inferred values of ion thermal conductivity (χ_i).*

Note that all power quantities include a calculation of equipartition power flow.

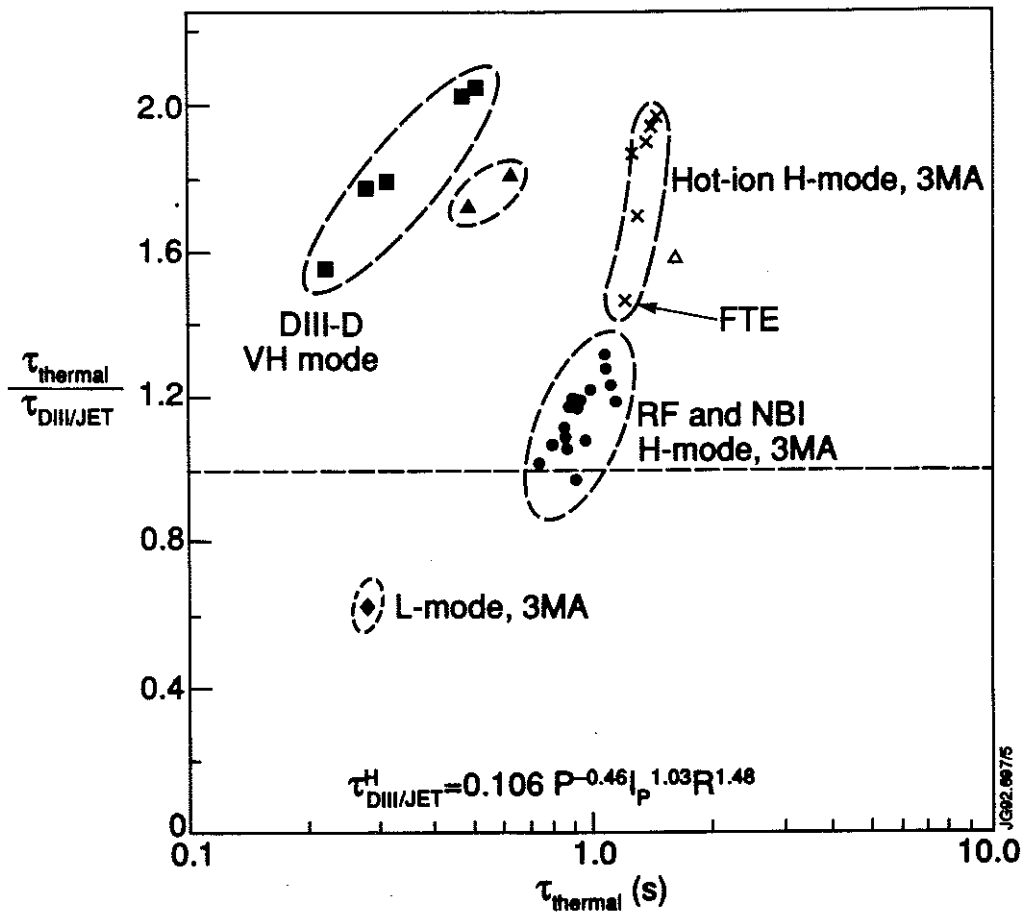

Fig. 8 *Thermal energy confinement times for JET Hot Ion H modes and other JET 3 MA H-modes normalised to the DIII-D/JET H-mode scaling. Also shown are JET H modes with high bootstrap current (I_{boot}/I_p~0.7) at 1-1.5 MA (▲) and the 3 MA PEP H-mode (△). The First Tritium Experiment shot is labelled 'FTE'.*

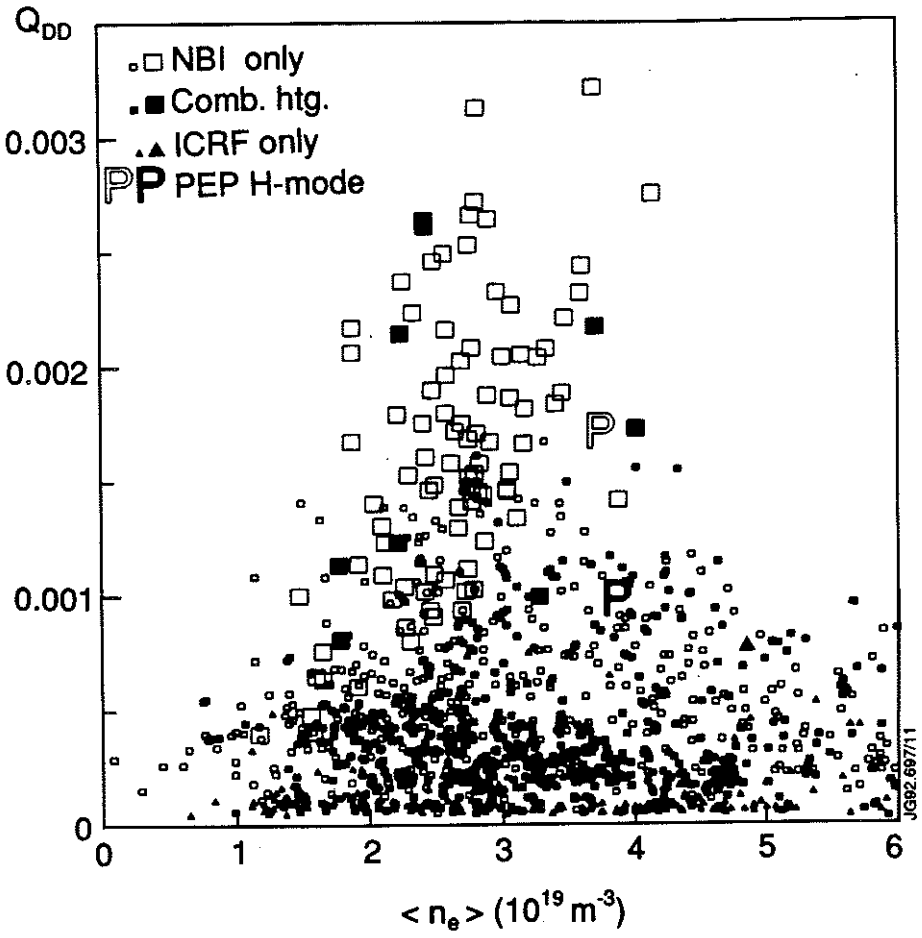

Fig. 9 *Fusion yield Q_{DD} as a function of volume are density for JET Deuterium plasmas with > 10 MW additional heating.*

Key to symbols:

□ □ *NBI heating only. Large symbols denote Hot Ion H modes*

■ ■ *Combined NBI/ICRF. Large symbols denote 'RF assisted' Hot Ion H-modes (all the HI H-modes have $P_{RF}/P_{TOT} < 1/3$).*

▲ *RF heating only. (Highest performance pulse is marked by a large triangle.)*

The 'P' symbols indicate the best PEP H-mode results. The open symbol (pulse 22624) has 10.6 MW NBI and 2 MW ICRF. The filled symbol (pulse 22490) has 8.8 MW ICRF and 2.6 MW NBI.

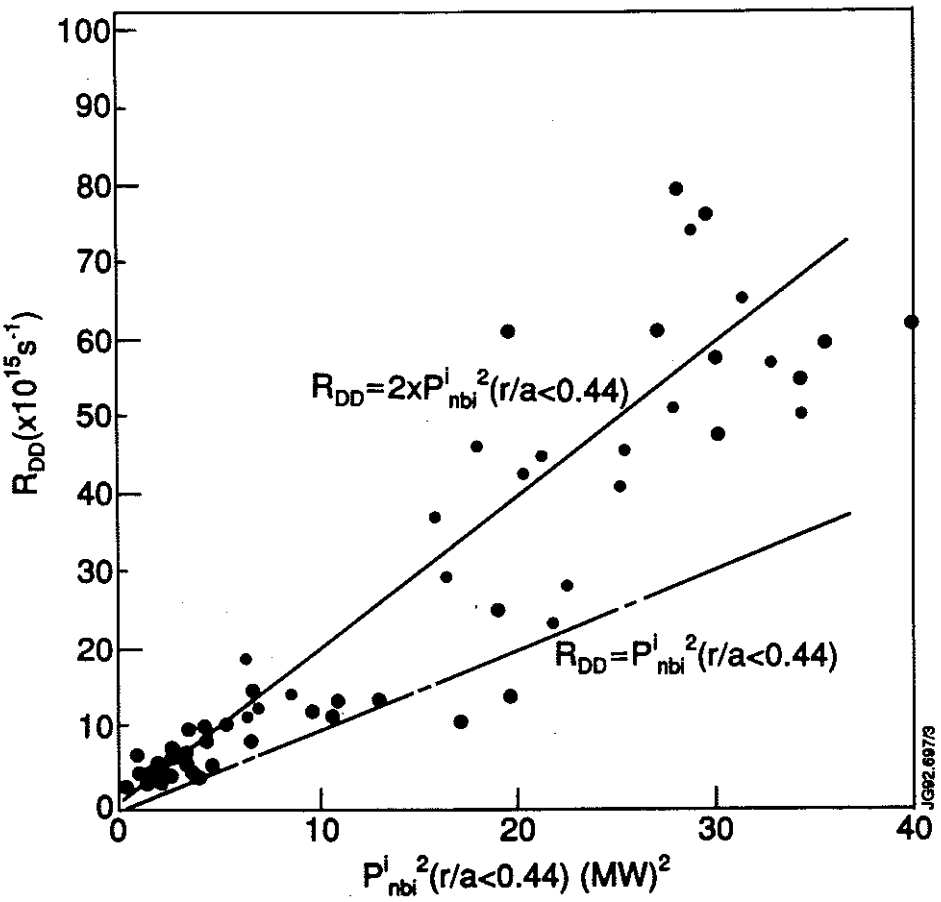

Fig. 10 *DD reaction rate plotted against NBI power deposited in the central 20% of the plasma volume for D° NBI heated plasmas.*

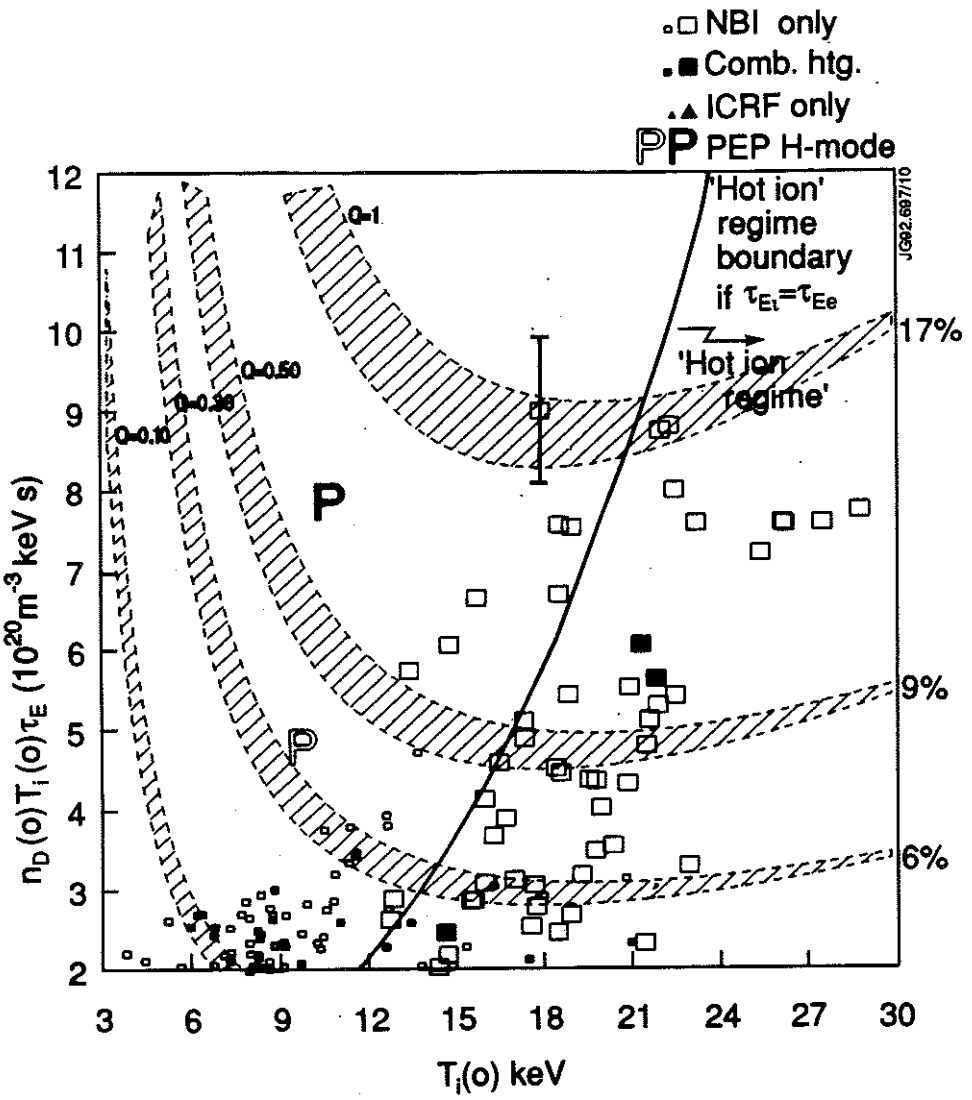

Fig. 11 *Triple fusion product ($n_D(o)$. T_i (o).τ_E) plotted against central ion temperature ($T_i(o)$) for the best JET plasmas with >10 MW additional heating. The line marked 'hot ion regime boundary' indicates the relationship defined in the text and in ref. 20. The symbolic representation is the same as in Fig. 9.*

The bars on the highest point represent the approximate accuracy of the quantities and applicable to all points.

Note that the 'Q' curves refer to equivalent 50:50 D-T plasmas in steady state and are only valid for broad parabolic profiles of density and temperature. Their comparison with the PEP H-modes is thus not strictly valid.

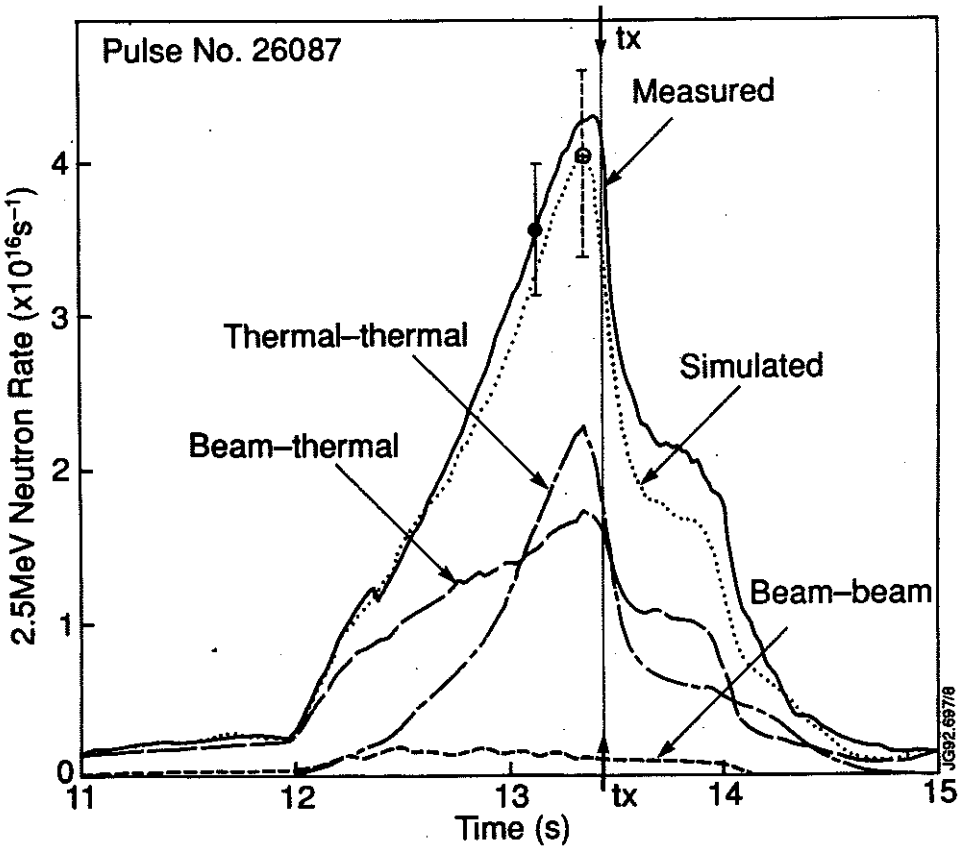

Fig. 12 *Measured and simulated neutron rates for 2.5 MeV neutrons for HI H mode pulse No. 26087. The time 't_X' indicates the collapse of the plasma performance accompanied by a strong influx of carbon impurity ('X' event). The high power (14.3 MW) NBI is applied at 12 s and switched off at 14 s.*

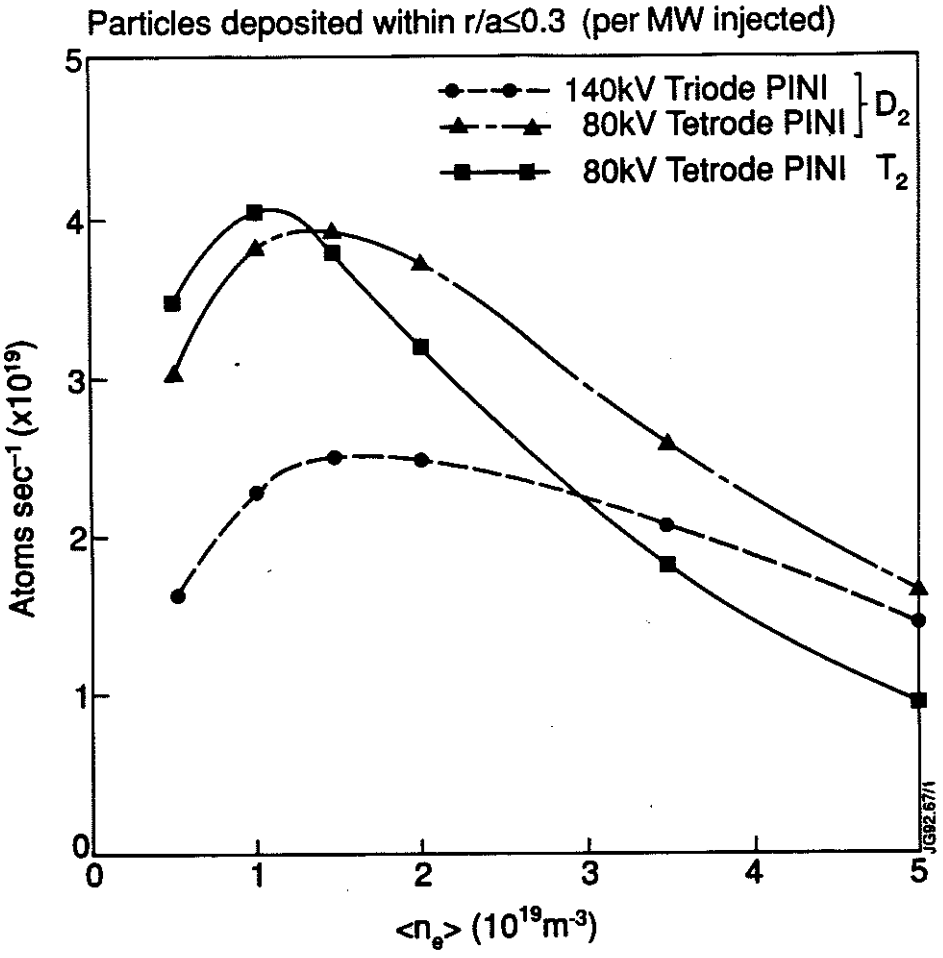

Fig. 13 *Computed fuelling rates per MW of injected bean power for the central 10% volume of a JET plasma with parabolic density profile (n_e (o)/< n_e > = 1.5) as a function of volume averaged density.*

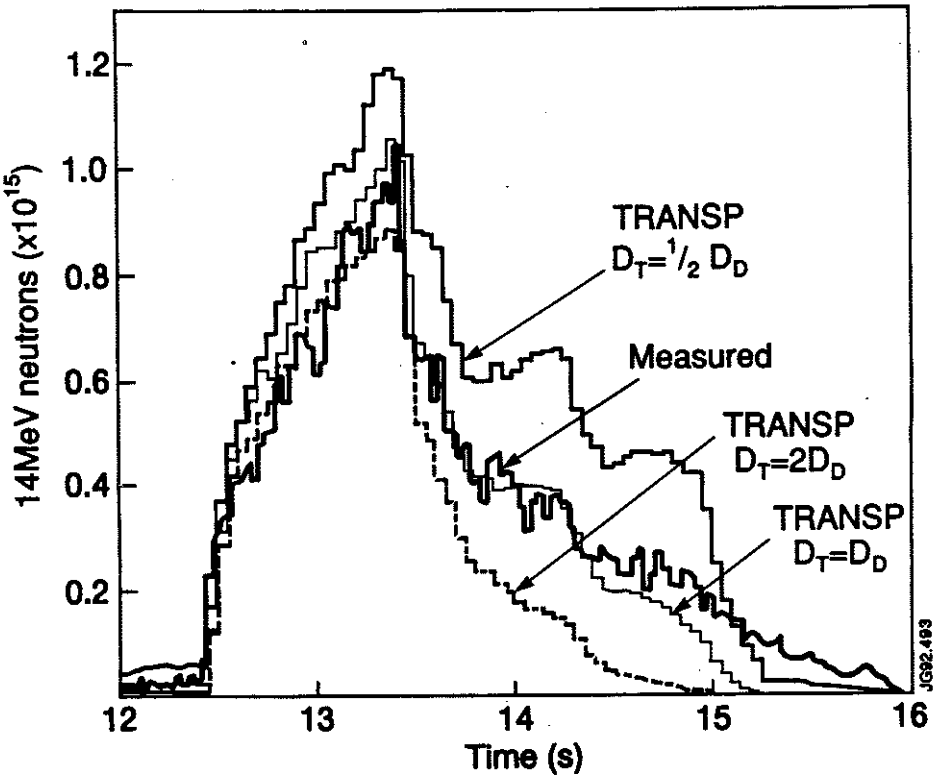

Fig. 14 *Measured 14 MeV neutron time profile during and after the injection of a '1% T in D' PINI beam from 12.5 - 13.5 s. The decay of the neutron profile is compared to TRANSP code simulations with various ratios of D_T/D_D.*

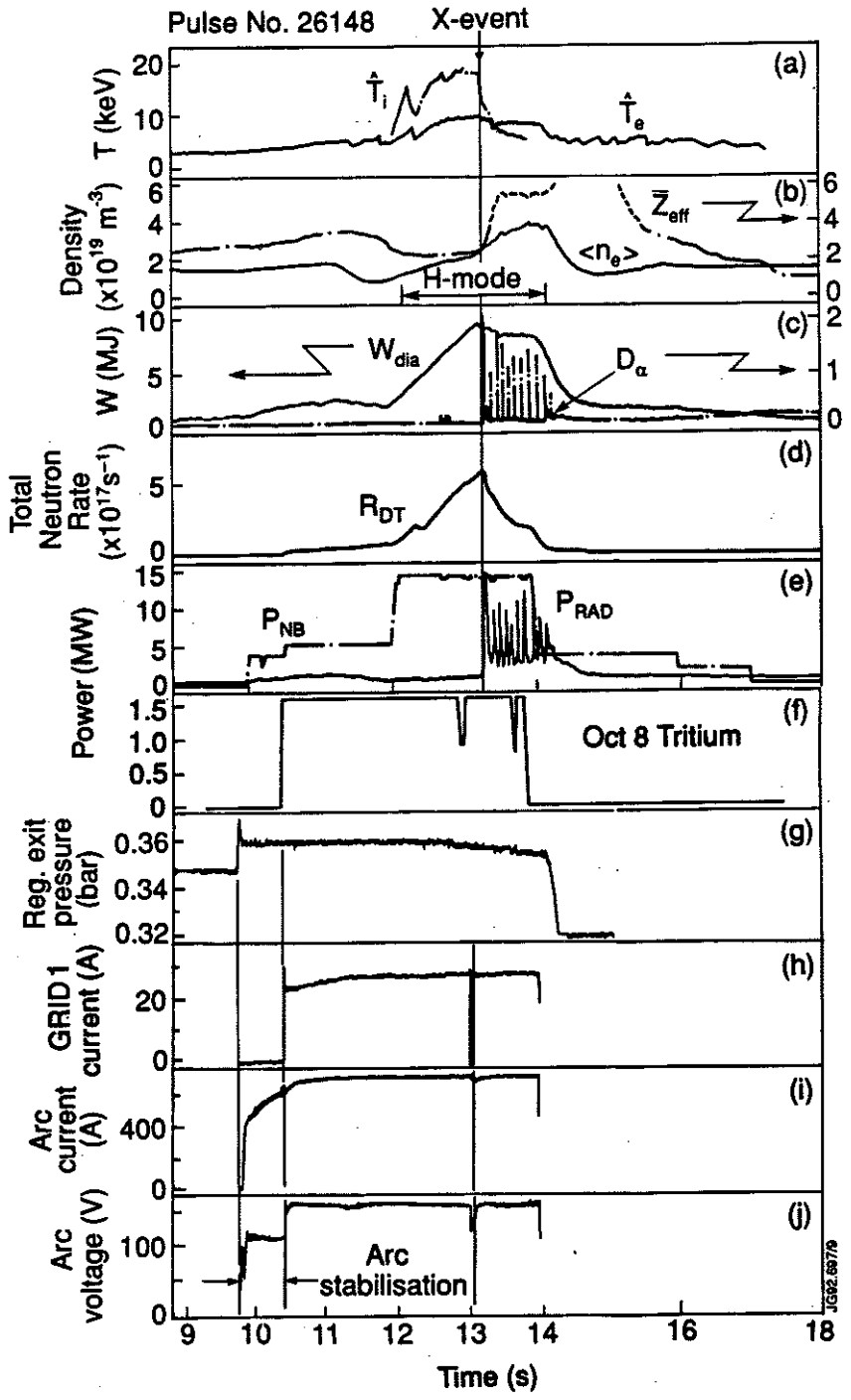

Fig. 15 *Time development of a JET FTE pulse No. 26148, producing 1.7 MW peak fusion power.*

(a) - (e) *Plasma parameters; central temperatures; volume averaged density; line averaged effective ion charge $\left(\bar{Z}_{eff}\right)$; plasma diamagnetic energy; D_α emission; total neutron rate and total input NBI power and radiated power.*

(f) *Tritium power input from NBI.*

(g) - (j) *Injector waveforms (gas, currents and voltages) of one of the tritium PINIs.*

Appendix I

THE JET TEAM

JET Joint Undertaking, Abingdon, Oxon, OX14 3EA, U.K.

J.M. Adams[1], B. Alper, H. Altmann, A. Andersen[14], P. Andrew, S.Ali-Arshad, W. Bailey, B. Balet, P. Barabaschi, Y. Baranov, P. Barker, R. Barnsley[2], M. Baronian, D.V. Bartlett, A.C. Bell, G. Benali, P. Bertoldi, E. Bertolini, V. Bhatnagar, A.J. Bickley, D. Bond, T. Bonicelli, S.J. Booth, G. Bosia, M. Botman, D. Boucher, P. Boucquey, M. Brandon, P. Breger, H. Brelen, W.J. Brewerton, H. Brinkschulte, T. Brown, M. Brusati, T. Budd, M. Bures, P. Burton, T. Businaro, P. Butcher, H. Buttgereit, C. Caldwell-Nichols, D.J. Campbell, D. Campling, P. Card, G. Celentano, C.D. Challis, A.V.Chankin[23], A. Cherubini, D. Chiron, J. Christiansen, P. Chuilon, R. Claesen, S. Clement, E. Clipsham, J.P. Coad, I.H. Coffey[24], A. Colton, M. Comiskey[4], S. Conroy, M. Cooke, S. Cooper, J.G. Cordey, W. Core, G. Corrigan, S. Corti, A.E. Costley, G. Cottrell, M. Cox[7], P. Crawley, O. Da Costa, N. Davies, S.J. Davies[7], H. de Blank, H. de Esch, L. de Kock, E. Deksnis, N. Deliyanakus, G.B. Denne-Hinnov, G. Deschamps, W.J. Dickson[19], K.J. Dietz, A. Dines, S.L. Dmitrenko, M. Dmitrieva[25], J. Dobbing, N. Dolgetta, S.E. Dorling, P.G. Doyle, D.F. Düchs, H. Duquenoy, A. Edwards, J. Ehrenberg, A. Ekedahl, T. Elevant[11], S.K. Erents[7], L.G. Eriksson, H. Fajemirokun[12], H. Falter, G. Fishpool, J. Freiling[15], C. Froger, P. Froissard, K. Fullard, M. Gadeberg, A. Galetsas, L. Galbiati, D. Gambier, M. Garribba, P. Gaze, R. Giannella, A. Gibson, R.D. Gill, A. Girard, A. Gondhalekar, D. Goodall[7], C. Gormezano, N.A. Gottardi, C. Gowers, B.J. Green, R. Haange, A. Haigh, C.J. Hancock, P.J. Harbour, N.C. Hawkes[7], N.P. Hawkes[1], P. Haynes[7], J.L. Hemmerich, T. Hender[7], J. Hoekzema, L. Horton, J. How, P.J. Howarth[5], M. Huart, T.P. Hughes[4], M. Huguet, F. Hurd, K. Ida[18], B. Ingram, M. Irving, J. Jacquinot, H. Jaeckel, J.F. Jaeger, G. Janeschitz, Z. Jankowicz[22], O.N. Jarvis, F. Jensen, E.M. Jones, L.P.D.F. Jones, T.T.C. Jones, J-F. Junger, F. Junique, A. Kaye, B.E. Keen, M. Keilhacker, W. Kerner, N.J. Kidd, R. Konig, A. Konstantellos, P. Kupschus, R. Lässer, J.R. Last, B. Laundy, L. Lauro-Taroni, K. Lawson[7], M. Lennholm, J. Lingertat[13], R.N. Litunovski, A. Loarte, R. Lobel, P. Lomas, M. Loughlin, C. Lowry, A.C. Maas[15], B. Macklin, C.F. Maggi[16], G. Magyar, V. Marchese, F. Marcus, J. Mart, D. Martin, E. Martin, R. Martin-Solis[8], P. Massmann, G. Matthews, H. McBryan, G. McCracken[7], P. Meriguet, P. Miele, S.F. Mills, P. Millward, E. Minardi[16], R. Mohanti[17], P.L. Mondino, A. Montvai[3], P. Morgan, H. Morsi, G. Murphy, F. Nave[27], S. Neudatchin[23], G. Newbert, M. Newman, P. Nielsen, P. Noll, W. Obert, D. O'Brien, J. O'Rourke, R. Ostrom, M. Ottaviani, S. Papastergiou, D. Pasini, B. Patel, A. Peacock, N. Peacock[7], R.J.M. Pearce, D. Pearson[12], J.F. Peng[26], R. Pepe de Silva, G. Perinic, C. Perry, M.A. Pick, J. Plancoulaine, J-P. Poffé, R. Pohlchen, F. Porcelli, L. Porte[19], R. Prentice, S. Puppin, S. Putvinskii[23], G. Radford[9], T. Raimondi, M.C. Ramos de Andrade, M. Rapisarda[29], P-H. Rebut, R. Reichle, S. Richards, E. Righi, F. Rimini, A. Rolfe, R.T. Ross, L. Rossi, R. Russ, H.C. Sack, G. Sadler, G. Saibene, J.L. Salanave, G. Sanazzaro, A. Santagiustina, R. Sartori, C. Sborchia, P. Schild, M. Schmid, G. Schmidt[6], H. Schroepf, B. Schunke, S.M. Scott, A. Sibley, R. Simonini, A.C.C. Sips, P. Smeulders, R. Smith, M. Stamp, P. Stangeby[20], D.F. Start, C.A. Steed, D. Stork, P.E. Stott, P. Stubberfield, D. Summers, H. Summers[19], L. Svensson, J.A. Tagle[21], A. Tanga, A. Taroni, C. Terella, A. Tesini, P.R. Thomas, E. Thompson, K. Thomsen, P. Trevalion, B. Tubbing, F. Tibone, H. van der Beken, G. Vlases, M. von Hellermann, T. Wade, C. Walker, D. Ward, M.L. Watkins, M.J. Watson, S. Weber[10], J. Wesson, T.J. Wijnands, J. Wilks, D. Wilson, T. Winkel, R. Wolf, D. Wong, C. Woodward, M. Wykes, I.D. Young, L. Zannelli, A. Zolfaghari[28], G. Zullo, W. Zwingmann.

PERMANENT ADDRESSES

1. UKAEA, Harwell, Didcot, Oxon, UK.
2. University of Leicester, Leicester, UK.
3. Central Research Institute for Physics, Budapest, Hungary.
4. University of Essex, Colchester, UK.
5. University of Birmingham, Birmingham, UK.
6. Princeton Plasma Physics Laboratory, New Jersey, USA.
7. UKAEA Culham Laboratory, Abingdon, Oxon, UK.
8. Universidad Complutense de Madrid, Spain.
9. Institute of Mathematics, University of Oxford, UK.
10. Freien Universität, Berlin, F.R.G.
11. Royal Institute of Technology, Stockholm, Sweden.
12. Imperial College, University of London, UK.
13. Max Planck Institut für Plasmaphysik, Garching, FRG.
14. Risø National Laboratory, Denmark.
15. FOM Instituut voor Plasmafysica, Nieuwegein, The Netherlands.
16. Dipartimento di Fisica, University of Milan, Milano, Italy.
17. North Carolina State University, Raleigh, NC, USA
18. National Institute for Fusion Science, Nagoya, Japan.
19. University of Strathclyde, 107 Rottenrow, Glasgow, UK.
20. Institute for Aerospace Studies, University of Toronto, Ontario, Canada.
21. CIEMAT, Madrid, Spain.
22. Institute for Nuclear Studies, Otwock-Swierk, Poland.
23. Kurchatov Institute of Atomic Energy, Moscow, USSR
24. Queens University, Belfast, UK.
25. Keldysh Institute of Applied Mathematics, Moscow, USSR.
26. Institute of Plasma Physics, Academica Sinica, Hefei, P. R. China.
27. LNETI, Savacem, Portugal.
28. Plasma Fusion Center, M.I.T., Boston, USA.
29. ENEA, Frascati, Italy.

At 1st July, 1992